Marine Chemistry 196 (2017) 62–70

Contents lists available at ScienceDirect

Marine Chemistry

journal homepage: www.elsevier.com/locate/marchem

# Molecular distribution and carbon isotope of *n*-alkanes from Ashtamudi Estuary, South India: Assessment of organic matter sources and paleoclimatic implications

Yadav Ankit[a], Praveen K. Mishra[b], Prem Kumar[a], Deepak K. Jha[c], Vivek V. Kumar[d], V. Ambili[e], Ambili Anoop[a,*]

[a] Indian Institute of Science Education and Research Mohali, Manauli, Punjab 140306, India
[b] Wadia Institute of Himalayan Geology, 33 GMS Road, Dehradun 248001, Uttarakhand, India
[c] Indian Institute of Science Education and Research Kolkata, Mohanpur, West Bengal 741246, India
[d] Geological Survey of India, Marine and Coastal Survey Division, Cochin, India
[e] Geological Survey of India, Marine and Coastal Survey Division, Visakhapatnam, India

ARTICLE INFO

*Keywords:*
Ashtamudi Estuary
Biomarkers
Carbon isotopes
*n*-alkanes
South India

ABSTRACT

The distribution and $\delta^{13}C$ composition of *n*-alkanes were used to identify organic matter (OM) sources in river dominated Ashtamudi Estuary, Southern India. A number of *n*-alkane indices have been calculated to illustrate the spatial variability by considering separately river dominated northern reaches and marine influenced southern part of the estuary. The carbon preference index (CPI) and average chain length (ACL) provide evidence for recycled organic inputs in the tidal zone, whereas dominant biogenic contribution has been observed in the riverine zone. The proxy ratio ($P_{aq}$) and terrigenous/aquatic ratio (TAR) indices demonstrate maximum aquatic productivity in the tidal dominated region of the Ashtamudi Estuary. The quantitative apportion of organic matter sources in Ashtamudi sediments using compound-specific carbon isotope analysis (CSIA) of long-chain *n*-alkane shows dominance (53–83%) of $C_3$ terrestrial plants derived OM. The results clearly demonstrate the effectiveness of an integrated molecular and stable carbon isotope analysis for quantitatively assessing OM sources in estuarine environments.

## 1. Introduction

Estuaries are highly productive and dynamic transitional ecosystem linking continental and marine environments (Bianchi, 2006). The pool of organic matter (OM) in estuaries comprises of riverborne allochthonous terrigenous materials and tidally advected marine allochthonous components which are mixed with autochthonous biomass derived production of marine organisms and intertidal vegetation (Burton and Liss, 1976; Thornton and McManus, 1994). The assessment of factors and processes that control sources and distribution of OM in estuarine sediments is important to understand the biogeochemical cycling and fate of terrigenous OM (e.g., Thornton and McManus, 1994; Harvey and Mannino, 2001; Middelburg and Herman, 2007; Fellman et al., 2009). The estuaries also preserve thick sequences of organic rich sediments that act as natural archive for global environment and sea-level changes (Müller, 2001; Bianchi and Allison, 2009). In spite of its importance, limited information (e.g., Jennerjahn et al., 2008; Sarma et al., 2011) has been available related to the sources and distribution of OM in tropical estuaries of Indian subcontinent.

The organic molecular biomarkers can provide abundant information about the sources of the organic matter, change in geochemical and biochemical processes as well as the information on past environmental changes (Eglinton and Hamilton, 1963; Poynter and Eglinton, 1990; Eglinton and Eglinton, 2008; He et al., 2014 and references therein). Lipid (*n*-alkanes) molecules are used to characterise OM in marine and terrestrial sediments owing to their relatively stable chemical property and low susceptibility to early diagenetic alteration (Meyers and Ishiwatari, 1993; Mead et al., 2005; Schouten et al., 2007; Wang et al., 2013 and references therein). The OM source identification using *n*-alkane has been conducted on the basis of carbon chain length variations specific to organic sources. The long-chain *n*-alkanes ($C_{27}$–$C_{33}$) are well known as a source indicator of terrestrial or land derived organic matter and short chain *n*-alkanes ($\leq C_{21}$) are attributed to algae and photosynthetic bacteria (Cranwell et al., 1987; Meyers, 2003). Furthermore, submerged and emergent aquatic plants are the main producers of mid-chain ($C_{21}$, $C_{23}$, and $C_{25}$) *n*-alkanes (Ficken et al., 2000).

* Corresponding author at: Indian Institute of Science Education and Research Mohali, Manauli, Punjab 140306, India.
*E-mail address:* anoop@iisermohali.ac.in (A. Anoop).

http://dx.doi.org/10.1016/j.marchem.2017.08.002
Received 6 February 2017; Received in revised form 11 June 2017; Accepted 4 August 2017
Available online 05 August 2017
0304-4203/ 

Several *n*-alkane indices have been developed to identify sources of OM in environments characterised by complex sources. The various *n*-alkane indices include (i) TAR (terrestrial/aquatic ratio), which approximates the proportions of long-chain (represent terrigenous sources of OM) to short-chain biomarkers (reflect aquatic sources) (Bourbonniere and Meyers, 1996), (ii) $P_{aq}$ (odd mid chain alkanes/odd mid and long chain alkanes), discriminate the relative contribution of non-emergent/emergent macrophytes and terrestrial vegetation using the relative proportion of mid chain to long chain homologues (Ficken et al., 2000), (iii) CPI (carbon preference index), odd/even predominance to determine the quality of soil OM and the contribution from sources such as terrestrial, microbial and/or petroleum hydrocarbons (e.g., Bray and Evans, 1961; Kolattukudy, 1976; Seki et al., 2006; Ahad et al., 2011), and (iv) average chain length (ACL), which describes average number of carbon atoms per molecule based on the abundance of the odd-carbon number higher plant derived *n*-alkanes (Poynter et al., 1989; Simoneit et al., 1991). However, the implementation of these *n*-alkane indices for OM source characterisation is questioned as their relationship with the controlling factors has long been debated and found to be region-specific (e.g., Bush and McInerney, 2013; Chevalier et al., 2015). For instance, the variations in *n*-alkane average chain length (ACL) could be interpreted in terms of changes in vegetation types (Cranwell, 1973; Schwark et al., 2002; Rommerskirchen et al., 2003), climate (Poynter et al., 1989; Simoneit et al., 1991; Sarkar et al., 2014), and contribution from petrogenic sources (Jeng, 2006; Ahad et al., 2011). Similarly, ambiguity is also associated with the usage of $P_{aq}$ index as submerged macrophytes have a tendency to increase production of long chain *n*-alkanes in shallow lakes during dry conditions (Aichner et al., 2010). The investigations on the linkage between local vegetation with *n*-alkane indices are extremely important for the OM source identification and application for paleoclimatic proxies.

The Ashtamudi Estuary, the second largest in Southern India, is characterised by unique biodiversity and hydrographic conditions with terrestrial mangrove forests dominate the upper estuary, while planktons/sea grasses as the marine end-members in the lower estuary. To assess the utility of biomarker (*n*-alkane) indices as means of assessing OM inputs to soils/sediments, a transect of sediment samples were taken from a terrestrial dominated upper estuarine area and a tidal influenced lower zone to determine the origin and transport of organic matter between the freshwater and marine end-members of these systems. Sediments, as well as dominant biomass components (modern vegetation) were analysed for lipid content and composition. Furthermore, $\delta^{13}C$ biomarker analyses of modern vegetation and surface sediments have also been conducted to assess the contribution of terrestrial vegetation ($C_3$ and $C_4$) in the Ashtamudi Estuary. The previous investigation of *n*-alkane biomarkers to assess organic matter sources from transition ecosystems in the Indian subcontinent has been limited to Pichavaram (Ranjan et al., 2015) and north of Kochi (Resmi et al., 2016). The major objectives of this work includes understanding the (i) physico-chemical (temperature, dissolved oxygen, alkalinity and salinity) characteristics of the Ashtamudi Estuary; (ii) the sources of organic matter by investigating lipid biomarker (*n*-alkanes) distribution in modern sediments and vegetation; (iii) validate the effectiveness of the *n*-alkane indices for source characterisation; and (iv) obtain a quantitative estimation of the OM source contribution using $\delta^{13}C$ biomarker and its implication for paleoclimate reconstruction.

## 2. Study area

### 2.1. Regional setting

The Ashtamudi Estuary is the second largest wetland system situated in the south coast of India (8°53′-9°02′ N, 76°31′-76°41′E) with a maximum extension of ca. 15 km in NE-SW direction (Fig. 1a). The Ashtamudi Estuary has been designated as a Ramsar Wetland of International Importance (Ramsar site no. 1204). The hydrological balance of the estuary is largely controlled by Kallada River (in the north) and the contribution from the south west (SW) and the north east (NE) monsoonal precipitation. The average annual discharge of the river is 2140 million $m^3$ with highest contributions during the monsoonal period (Sajan et al., 1992). The lower end of the estuary opens to the Arabian Sea through a relatively narrow channel (ca. 200 m) (Qasim, 2003).

Morphologically, the region is characterised by gently sloping valleys, coastal plains, channel fill deposits and tidal flats (Nair et al., 2010). The catchment of the Ashtamudi Estuary is marked by Tertiary and Quaternary sediments with Archean crystalline basement (Nair et al., 2010; Padmalal et al., 2011). The Quaternary sediments of the region comprises of coastal sands and alluviums distributed all along the coastal plains and valleys.

### 2.2. Regional climate and vegetation

The climate over western coast of India is mainly tropical in nature administered by SW monsoon between June and September, and NE monsoon during October to December. The precipitation (2004–2014 CE) data from the study area reveals that the region receives an average annual rainfall of ~2400 mm with ~52% contribution from the SW monsoon and ~26% from NE monsoon (source: Indian Meteorological Department). The average temperature of the region varies between 26 °C (during June/July) and 36 °C (during April/May).

The Ashtamudi Estuary is located within the Southern Tropical Moist Deciduous Forest biome (Champion and Seth, 1968). The modern vegetation in Ashtamudi region is characterised by $C_3$ plants as the major representatives of the flora. The dominant portion of the Kallada drainage basin is occupied by natural forests and cultivated lands comprising of teak and tea (Jennerjahn et al., 2008). The $C_3$ vegetation of the region comprises of herbs (181 species, accounts for ~71% of all the plant species), climbers (25 species, ~10% of all the plant species), shrubs (19 species, ~8% of all the plant species) and trees (31 species, ~ 12% of all the plant species) (Sabu and Ambat, 2007). The prominent tree growths in the region constitute of *Thespesia populnea, Cocos nucifera, Arecaceae* and *Magnifera indica*. The upper estuary is dominated by mangrove vegetation comprising of *Sonneratia alba, Acanthus ilicifolius, Acrostichum aureum, Avicennia officinalis* and *Brugiera gymnorrhiza* (Krishnan et al., 2014; Sumesh et al., 2014).

### 2.3. Sedimentological, physicochemical and biological characteristics

The sediment distribution in Ashtamudi Estuary is characterised by (i) sand/gravel dominated estuarine head, (ii) mud dominated sediments in the central part of basin and (iii) tidally advected sand in the lower estuary mouth (Sajan et al., 1992; Anooja et al., 2013). The physicochemical parameters and dissolved nutrients varied both seasonally and longitudinally along the course of Ashtamudi Estuary (Nair et al., 1984; Sujatha et al., 2009; Babu et al., 2010; Antony and Ignatius, 2016). The average annual gross productivity in the surface water was maximum (148.09 mgC/$m^3$/h) nearest to the marine zone (Neendakara) and minimum (103.62 mgC/$m^3$/h) towards the riverine zone (Nair et al., 1984). The faunal density was higher in the lower part of the estuary with peak abundance during the monsoon season (Divakaran et al., 1981). Similarly, the phytoplankton abundance increased from 47 cells $l^{-1}$ near the river mouth to 121 × $10^3$ cells $l^{-1}$ in the tidal dominated lower estuary (Jennerjahn et al., 2008).

In Ashtamudi sediments, the $C_{org}$ values varied between 0.3 and 3.5% (Jennerjahn et al., 2008). The $\delta^{13}C_{org}$ value in the Ashtamudi sediments show lowest values close to riverine zone (−25.9 to −22.7‰), whereas higher values (−24.3 to −20.9‰) are observed towards the marine influenced lower estuary (Jennerjahn et al., 2008).

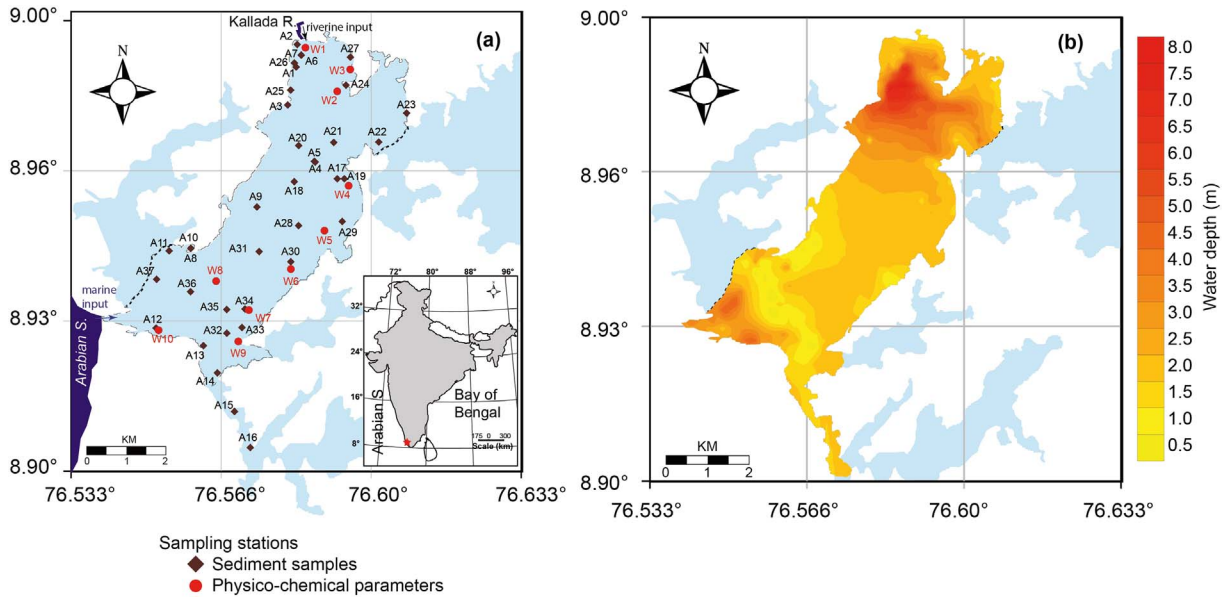


**Fig. 1.** (a) Map of study area including sampling locations of sediment and physico-chemical parameters. (b) Bathymetry of the basin.

## 3. Material and methods

### 3.1. Sampling

#### 3.1.1. Collection of modern vegetation and surface sediment samples

The bathymetric survey over the study area was carried out using a portable echo sounder – South SDE-28 Single Frequency Digital Echosounder with a frequency of 200 kHz. The physico-chemical properties like pH, temperature, conductivity, salinity and dissolved oxygen were measured from ten representative locations in Ashtamudi Estuary (Fig. 1a). The *n*-alkane analyses were conducted on sediment samples ($n$ = 37) covering the main central part of the Ashtamudi Estuary collected using a Wildco Ponar type grab sampler with a maximum penetration depth of about 5–7 cm. Additionally, leaves of the most abundant plant species from the Ashtamudi Estuary has been collected for lipid extraction to understand potential carbon sources. The plants species were identified at the lowest taxonomic level (Supplementary material Table S1). All samples, sediment and vegetation, were oven dried and ground finely prior to extraction.

### 3.2. Analytical methods

#### 3.2.1. Lipid extraction

The lipid content of modern vegetation (~0.3 mg) and sediment samples (ca. 10–15 g) was extracted using accelerated solvent extractor (Dionex ASE 350) with dichloromethane/methanol (93:7) at 100 °C and 1600 psi for 2 cycles. Sample preparation and lipid extraction methods have been described in detail elsewhere (Samanta et al., 2013; Basu et al., 2017; Ghosh et al., 2017). All solvents used in the study, i.e., *n*-hexane (HEX), dichloromethane (DCM) and methanol (MeOH), were of HPLC grade (Merck, Darmstadt, Germany). A surrogate standard (5-alpha-androstane from Sigma-Aldrich) was used to determine percent recovery of alkanes. The aliphatic hydrocarbon fraction containing *n*-alkane was separated from the total lipid extract (TLE) using activated silica gel column (100–200 mesh) eluted with *n*-hexanes. The alkene fractions were not separated from the aliphatic hydrocarbons. Aliphatic hydrocarbons (*n*-alkanes) were identified and quantified by gas chromatography-flame ionization detector (Agilent 7890A, HP-5MS column, 30 m × 250 μm × 0.25 μm) after injection of 1 μl of sample. The GC-oven temperature was started at 60 °C and increased to 320 °C at 8 °C/min, and held at 320 °C for 12 min. The *n*-alkane homologues were identified by comparison with spectra obtained after running Supelco alkane-mixture standard ($C_{10}$–$C_{40}$).

#### 3.2.2. Compound-specific $\delta^{13}C$ analyses

The stable isotope ($\delta^{13}C$) composition of *n*-alkanes was measured in GC system (Thermo Trace Ultra GC) coupled via combustion interface (GC-Isolink) to a Thermofisher Scientific (MAT 253) isotope ratio mass spectrometer (GC-IRMS). The GC oven temperature was started at 40 °C (1 min) to 320 °C (held 12 min) with ramp of 10 °C/min. The *n*-alkanes individual compounds were combusted in presence of $O_2$ with He (1% v/v) at 950 °C to produce $CO_2$. The evolved $CO_2$ was sent to IRMS to measure isotope ratios. Calibration of isotope analysis was performed by injecting several pulses of $CO_2$ at the beginning and at the end of each GC run and by measurement of certified standards between sample runs. The standard deviation for specific compounds was better than 0.5‰, based on at least duplicate analyses. Isotopic ratios are expressed as $\delta^{13}C$ values in per mil relative to the Vienna Pee Dee Belemnite (V-PDB) standard. A standard mixture (A5) of *n*-alkanes ($C_{16}$–$C_{30}$), provided by A. Schimmelmann of Indiana University, with a known isotopic composition was used daily to monitor the precision and accuracy of measurements. Standard deviations for replicates of all measured compounds are listed in Table 2.

## 4. Results

### 4.1. Bathymetry and physicochemical parameters

The hydrographic survey conducted in Ashtamudi Estuary shows an average water depth of ~2.26 m with a vent shaped depression in the proximity of Kallada River (Fig. 1b). The maximum depth (~9.12 m) was noted in the upper end of the estuary near the mouth of the Kallada River (Fig. 1b). The bathymetric contours reveals minimum depth (0.15 m) in the lower estuary with development of sandy islands due to high input of tidally advected littoral sediments.

The physicochemical parameters of Ashtamudi Estuary are listed in Table S2 (Supplementary material). The surface water temperature of the Ashtamudi Estuary during the study period ranges from 26.5 to 29.3 °C. The salinity varied from 1.9 to 3.3 ppt (average = 2.8 ppt) with salinity gradient increasing towards the mouth of the lagoon. The pH of the water samples from Ashtamudi Estuary ranges from 8.38 to 8.65 with an average value of 8.47, indicating alkaline nature of the water. The dissolved oxygen in the Ashtamudi estuary ranges from 6.22 to 7.48 mg/l with maximum values observed towards the lower estuary

**Table 1**
Concentrations and *n*-alkane parameters of the Ashtamudi surface sediments.

| Sample name | CPI | $P_{aq}$ | TAR | ACL | *n*-alkane conc. (μg/g) | Short chain (%) | Mid chain (%) | Long chain (%) |
|---|---|---|---|---|---|---|---|---|
| A1 | 3.8 | 0.10 | 11.8 | 30.3 | 6.0 | 5.5 | 8.9 | 85.6 |
| A2 | 3.4 | 0.12 | 5.5 | 30.3 | 2.2 | 10.3 | 10.8 | 78.9 |
| A3 | 3.3 | 0.12 | 9.3 | 30.3 | 3.3 | 6.6 | 10.5 | 82.9 |
| A4 | 2.5 | 0.12 | 7.9 | 30.3 | 2.9 | 7.6 | 10.3 | 82.2 |
| A5 | 2.4 | 0.16 | 8.0 | 30.0 | 1.3 | 6.9 | 14.2 | 78.9 |
| A6 | 2.9 | 0.12 | 7.2 | 30.2 | 2.8 | 8.5 | 10.4 | 81.1 |
| A7 | 1.8 | 0.26 | 1.8 | 29.4 | 1.0 | 18.5 | 16.4 | 65.0 |
| A8 | 2.4 | 0.26 | 4.7 | 29.2 | 2.1 | 17.7 | 18.6 | 63.7 |
| A9 | 1.3 | 0.32 | 1.4 | 29.1 | 0.7 | 17.7 | 16.3 | 65.9 |
| A10 | 1.1 | 0.36 | 1.2 | 28.8 | 0.9 | 28.1 | 18.2 | 53.7 |
| A11 | 1.2 | 0.40 | 1.3 | 28.5 | 0.8 | 27.5 | 24.8 | 47.7 |
| A12 | 2.5 | 0.23 | 1.8 | 29.5 | 1.7 | 20.8 | 16.4 | 62.8 |
| A13 | 1.9 | 0.27 | 2.0 | 29.3 | 1.0 | 21.3 | 20.0 | 58.8 |
| A14 | 2.5 | 0.16 | 4.6 | 29.9 | 2.2 | 11.5 | 13.4 | 75.1 |
| A15 | 3.1 | 0.12 | 7.6 | 30.2 | 2.8 | 8.0 | 10.5 | 81.5 |
| A16 | 1.7 | 0.31 | 3.2 | 29.0 | 2.3 | 9.7 | 15.3 | 75.0 |
| A17 | 3.3 | 0.11 | 9.2 | 30.3 | 4.7 | 10.0 | 9.8 | 80.2 |
| A18 | 2.8 | 0.12 | 8.6 | 30.3 | 3.7 | 9.9 | 9.7 | 80.4 |
| A19 | 3.1 | 0.12 | 11.0 | 30.3 | 3.0 | 10.9 | 9.7 | 79.5 |
| A20 | 3.2 | 0.11 | 11.7 | 30.4 | 4.5 | 11.5 | 9.4 | 79.1 |
| A21 | 3.2 | 0.11 | 6.4 | 30.4 | 4.2 | 12.7 | 11.3 | 76.0 |
| A22 | 3.2 | 0.12 | 7.9 | 30.2 | 2.6 | 14.8 | 10.8 | 74.4 |
| A23 | 3.2 | 0.15 | 6.7 | 30.1 | 2.6 | 13.0 | 12.5 | 74.5 |
| A24 | 3.4 | 0.09 | 11.2 | 30.5 | 2.1 | 7.7 | 8.6 | 83.7 |
| A25 | 2.5 | 0.20 | 2.7 | 29.7 | 1.2 | 16.8 | 14.9 | 68.3 |
| A26 | 3.9 | 0.11 | 9.0 | 30.3 | 4.2 | 9.9 | 10.3 | 79.8 |
| A27 | 3.9 | 0.10 | 12.2 | 30.5 | 6.6 | 10.8 | 8.9 | 80.4 |
| A28 | 3.0 | 0.12 | 8.3 | 30.3 | 4.1 | 10.0 | 9.4 | 80.6 |
| A29 | 3.2 | 0.11 | 8.6 | 30.3 | 3.6 | 10.4 | 9.4 | 80.2 |
| A30 | 3.6 | 0.11 | 11.1 | 30.3 | 5.1 | 8.8 | 9.3 | 81.9 |
| A31 | 3.2 | 0.11 | 10.7 | 30.3 | 4.5 | 9.7 | 9.3 | 81.0 |
| A32 | 2.2 | 0.18 | 3.9 | 29.9 | 1.7 | 16.7 | 13.9 | 69.3 |
| A33 | 3.1 | 0.14 | 7.1 | 30.1 | 3.9 | 12.9 | 11.7 | 75.4 |
| A34 | 2.8 | 0.13 | 6.2 | 30.2 | 1.9 | 12.2 | 10.8 | 77.0 |
| A35 | 1.9 | 0.19 | 3.4 | 29.8 | 0.7 | 16.7 | 13.3 | 70.0 |
| A36 | 1.5 | 0.27 | 2.0 | 29.3 | 0.4 | 16.7 | 15.4 | 67.9 |
| A37 | 2.8 | 0.17 | 5.3 | 29.9 | 2.4 | 15.3 | 12.6 | 72.1 |

Note: $P_{aq.} = (C_{23} + C_{25}) / (C_{23} + C_{25} + C_{31} + C_{33})$, $TAR = (C_{27} + C_{29} + C_{31}) / (C_{15} + C_{17} + C_{19})$, $CPI = [\Sigma(C_{25} - C_{33})_{odd} / \Sigma (C_{24} - C_{32})_{even} + \Sigma (C_{25} - C_{33})_{odd} / \Sigma (C_{26} - C_{34})_{even}] / 2$, $ACL = (23 \times C_{23} + 25 \times C_{25} + 27 \times C_{27} + 29 \times C_{29} + 31 \times C_{31}) / (C_{23} + C_{25} + C_{27} + C_{29} + C_{31})$, Short Chain % = $[\Sigma (C_{14} - C_{20}) / \Sigma (C_{14} - C_{40})] * 100$, Mid Chain % = $[\Sigma (C_{21} - C_{26}) / \Sigma (C_{14} - C_{40})]$, Long Chain % = $[\Sigma (C_{27} - C_{40}) / \Sigma (C_{14} - C_{40})] * 100$.

(W8, Neendakara station).

### 4.2. n-alkane distribution of modern vegetation and surface sediments

The *n*-alkane distributions of modern vegetation ($C_3$ and $C_4$) from Ashtamudi region showed dominance of long chain ($C_{27}$–$C_{33}$) homologues diagnostic of land-plant waxes (Supplementary material S3). The abundance and distribution of *n*-alkane were similar for trees ($C_3$) and grasses ($C_4$). The relative abundance of *n*-alkanes in Ashtamudi sediments is shown in Table 1. The long-chain *n*-alkanes ranging from $C_{21}$ to $C_{35}$ are the dominant constituents in all the surface sediments (Fig. 2a). The total concentrations of $C_{15}$–$C_{35}$*n*-alkanes in Ashtamudi Estuary sediments varied from 0.42 to 6.6 μg/g (Fig. 2b). The relative abundance of *n*-alkanes in the surface sediments showed a strong odd-over-even preference and were dominated by either $C_{29}$ or $C_{31}$ homologues (Supplementary material S3).

### 4.2. n-alkane indices

The CPI index of the Ashtamudi surface sediments varied from 1.1 to 3.9, whereas the ACL value ranged from 28.5 to 30.5 (Table 1). The ACL and CPI values showed pronounce decreasing trend towards lower estuary (Fig. 3a and b). The highest CPI was observed at the most up-river site (A 26 and A 27; CPI ~ 3.9), and the lowest CPI (A 10; CPI ~ 1.1) was found in sediments collected near the lower estuary. Sediments collected near the lower end of estuary exhibited the lowest ACL value (A 11, ~28.5), whereas the highest ACL (A24, ~30.5) was found at location close to the river mouth. The CPI and ACL values of the surface sediments from the Ashtamudi Estuary shows high correlation ($r = 0.91$, $n = 37$; $p < 0.05$).

The TAR values of the Ashtamudi sediments ranged from 1.2 to 12.2 denoting the predominance of terrigenous sources of *n*-alkanes. The higher TAR values have been observed towards the upper Estuary (Fig. 3c). The $P_{aq}$ values of the Ashtamudi estuarine sediments ranged between 0.1 and 0.4 with higher values observed towards the proximity of the open sea (Fig. 3d). The TAR and $P_{aq}$ of Ashtamudi Estuary are significantly correlated ($r = -0.85$; $n = 37$; $p < 0.05$) (Supplementary material Fig. S4).

### 4.3. $\delta^{13}C$ of n-alkanes in surface sediments

The carbon isotope measurements were performed on fifteen surface sediments and twelve modern vegetation samples. The compound-specific isotope ($\delta^{13}C$) values for the modern vegetation were reported for the n-$C_{29}$ and n-$C_{31}$ homologues since these compounds were found in higher abundances than those of other long chain alkanes. The modern $C_3$ vegetation from the Ashtamudi region was characterised by $\delta^{13}C$ values of $-36.2 \pm 1.5$‰ and $-36.9 \pm 1.5$‰ for $C_{29}$ and $C_{31}$ component respectively. The *n*-alkane $\delta^{13}C$ values of modern $C_4$ plants were $-21.2 \pm 2.0$‰ and $-21.0 \pm 1.9$‰ for $C_{29}$ and $C_{31}$ respectively.

The long-chain *n*-alkane $\delta^{13}C$ signatures for the surface sediments from the Ashtamudi estuary ranged from $-29.5$ to $-34.2$‰ (Table 2). Long-chain *n*-alkane $\delta^{13}C$ values of n-$C_{31}$ homolog is positively correlated with n-$C_{29}$ ($r = 0.64$; $n = 15$; $p < 0.05$) and n-$C_{33}$ ($r = 0.75$; $n = 15$; $p < 0.05$). Therefore, only spatial distribution in $\delta^{13}C$ for the n-$C_{31}$ will be discussed further. The $\delta^{13}C_{C31}$ values fluctuates from $-29.5$ to $-34.2$‰ with an average of $-32.0 \pm 1.3$‰. The $\delta^{13}C_{C31}$ showed a downriver $^{13}C$-enrichment of around 3–4‰.

## 5. Discussion

### 5.1. Physicochemical charactersitics of Ashtamudi Estuary

The physicochemical parameters varied seasonally along the course of Ashtamudi Estuary influenced by river influx and tidal intrusion. The salinity of the Ashtamudi Estuary decreased towards the upper end due to its proximity to the Kallada River. The dissolved oxygen acts as a catalyst to regulate the different metabolic processes of various organisms and indicates the trophic status and magnitude of eutrophication (Johannessen and Dahl, 1996). The high rate of primary production by phytoplantktons and benthic macro algae may be accounted for high dissolved oxygen at the marine zone (Nair et al., 1984). The variation in pH shows no pronounced changes along the course of the Ashtamudi Estuary. However, the slight decrease in pH observed in the tidal influenced lower estuary could be explained in terms of significant organic matter decomposition resulting in the lowering of pH (Saran and Adoni, 1982; Sarma et al., 2011).

### 5.2. n-alkane indices for OM source characterisation

#### 5.2.1. Estimation of terrigenous versus recycled OM

The CPI index based on odd over even predominance of long-chain *n*-alkanes distribution have been widely used to trace OM sources (e.g., Bush and McInerney, 2013). The terrestrial plant waxes generally have high (> 3) CPI values (Rieley et al., 1991; Hedges and Prahl, 1993), whereas *n*-alkanes from petrogenic inputs have CPI values close to 1.0 (Farrington and Tripp, 1977). CPI values close to unity further indicate

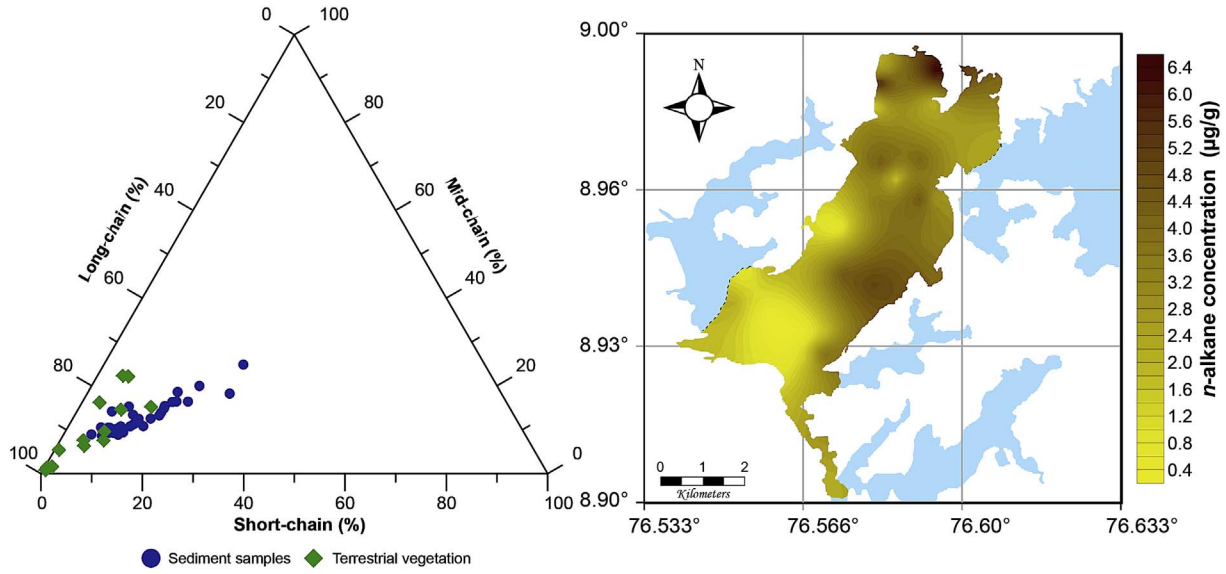


**Fig. 2.** (a) Ternary diagram of short, mid and long-chain *n*-alkane concentrations in modern vegetation and surface sediments. (b) Spatial distributions of *n*-alkanes concentrations in surface sediments.

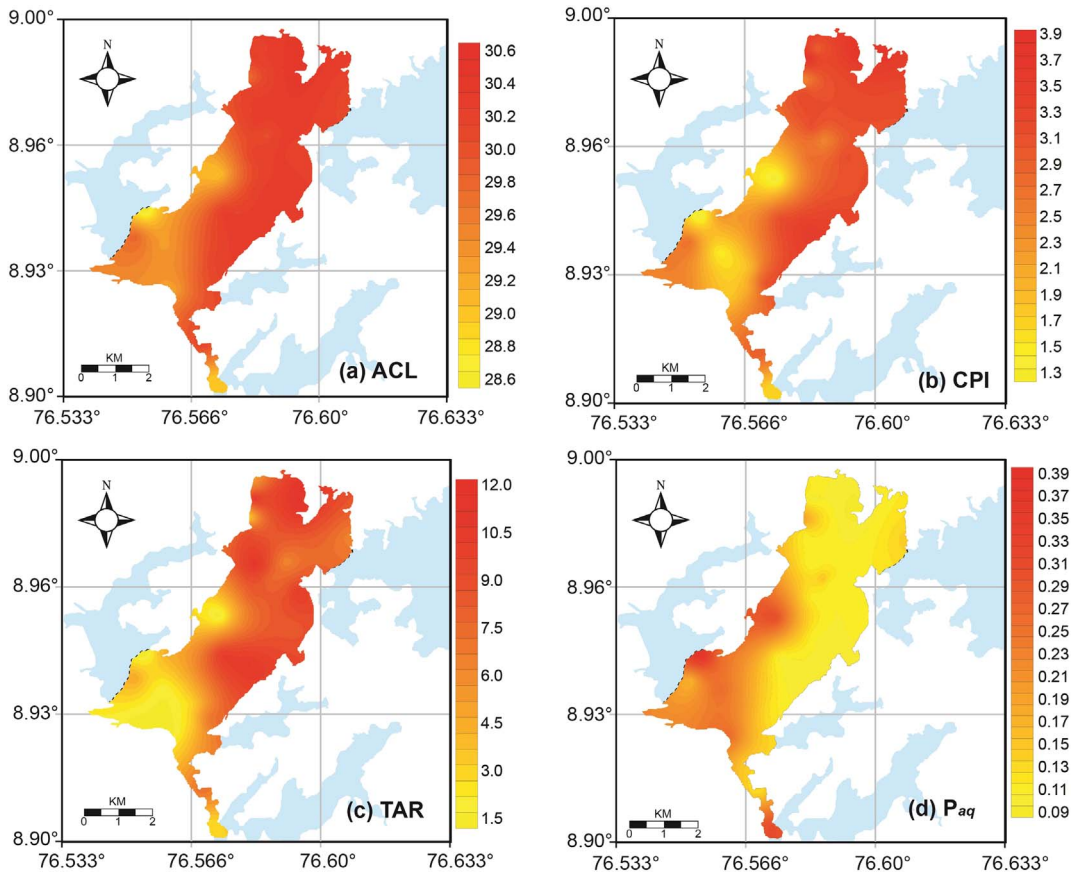


**Fig. 3.** Spatial distribution of *n*-alkane indices (a) ACL, (b) CPI, (c) TAR and (d) $P_{aq}$.

greater input from marine microorganisms and/or recycled organic matter (Kennicutt et al., 1987). Conversely, the ACL values are potentially useful parameter for climate-dependent vegetation change (Rommerskirchen et al., 2003; Sarkar et al., 2014). The vegetation in drier and warmer climates biosynthesise longer chain alkyl lipids than plants in habitats of temperate regions (Gagosian and Peltzer, 1986). Additionally, the ACL has also been used to differentiate marine and fluvial sediments as the values are significantly lowered if petrogenic hydrocarbons were added to sediments containing biogenic hydrocarbons (Jeng, 2006). The CPI index in Ashtamudi Estuary exhibit similar spatial pattern that mirror ACL values (Fig. 3a and b). The relatively high CPI and ACL values observed in the upper Ashtamudi estuary are typical for sediments dominated by terrestrial vascular plants, whereas the low CPI and ACL in the tidal influenced marine zone indicates significant recycled organic input (Fig. 3a and b). This inference has also been corroborated by exceptionally high $\delta^{15}N$ values

**Table 2**
Compound specific $\delta^{13}C$ values for the long chain *n*-alkanes of modern vegetation and sediment samples from Ashtamudi Estuary.

| | Sample name | $\delta^{13}C_{27}$ (‰) | $\delta^{13}C_{29}$ (‰) | $\delta^{13}C_{31}$ (‰) | $\delta^{13}C_{33}$ (‰) |
|---|---|---|---|---|---|
| Sediments samples | A1 | − 32.0 ± 0.2 | − 33.5 ± 0.3 | − 33.9 ± 0.3 | − 33.8 ± 0.3 |
| | A11 | − 30.3 ± 0.2 | − 31.1 ± 0.3 | − 33.4 ± 0.2 | − 31.8 ± 0.2 |
| | A12 | − 31.2 ± 0.3 | − 31.1 ± 0.3 | − 29.5 ± 0.3 | − 31.0 ± 0.4 |
| | A14 | − 30.4 ± 0.2 | − 30.8 ± 0.4 | − 30.2 ± 0.3 | − 31.6 ± 0.2 |
| | A17 | − 29.4 ± 0.4 | − 31. ± 0.3 | − 31.0 ± 0.4 | − 31.4 ± 0.3 |
| | A18 | − 30.8 ± 0.3 | − 31.8 ± 0.2 | − 31.6 ± 0.3 | − 30.9 ± 0.3 |
| | A19 | − 31.4 ± 0.3 | − 32.1 ± 0.2 | − 31.9 ± 0.4 | − 31.9 ± 0.4 |
| | A20 | − 30.9 ± 0.2 | − 30.9 ± 0.2 | − 32.4 ± 0.2 | − 31.1 ± 0.3 |
| | A22 | − 29.1 ± 0.3 | − 30.8 ± 0.3 | − 31.9 ± 0.4 | − 31.6 ± 0.3 |
| | A24 | − 31.7 ± 0.2 | − 33.3 ± 0.2 | − 34.2 ± 0.3 | − 32.9 ± 0.3 |
| | A28 | − 31.8 ± 0.2 | − 31.7 ± 0.2 | − 32.3 ± 0.3 | − 31.5 ± 0.2 |
| | A29 | | − 31.5 ± 0.4 | − 31.8 ± 0.3 | − 31.5 ± 0.3 |
| | A30 | − 31.6 ± 0.3 | − 31.9 ± 0.2 | − 32.7 ± 0.4 | − 32.0 ± 0.3 |
| | A35 | − 31.2 ± 0.4 | − 32.7 ± 0.3 | − 31.9 ± 0.3 | − 31.6 ± 0.4 |
| | A36 | − 32.8 ± 0.3 | − 31.2 ± 0.3 | − 30.5 ± 0.2 | − 30.1 ± 0.3 |
| $C_4$ plants | AE1 | − 21.8 ± 0.4 | − 20.9 ± 0.3 | − 19.5 ± 0.3 | − 19.5 ± 0.2 |
| | AE3 | − 22.0 ± 0.2 | − 23.3 ± 0.3 | − 23.0 ± 0.2 | − 22.3 ± 0.2 |
| | AE7 | − 21.7 ± 0.2 | − 22.5 ± 0.2 | − 22.7 ± 0.2 | − 21.6 ± 0.2 |
| | AE8 | − 20.3 ± 0.3 | − 21.2 ± 0.3 | − 21 ± 0.4 | − 19.9 ± 0.3 |
| | AE9 | − 21.8 ± 0.2 | − 18.1 ± 0.2 | − 18.7 ± 0.2 | − 20.6 ± 0.2 |
| $C_3$ plants | AE2 | | − 36.5 ± 0.3 | − 37.7 ± 0.3 | − 36.4 ± 0.4 |
| | AE5 | − 33.1 ± 0.2 | − 33.3 ± 0.2 | − 34.0 ± 0.3 | − 34.3 ± 0.3 |
| | AE6 | − 35.3 ± 0.2 | − 35.9 ± 0.2 | − 36.6 ± 0.2 | − 35.1 ± 0.3 |
| | AE10 | − 35.4 ± 0.4 | − 36.2 ± 0.2 | − 36.8 ± 0.4 | − 35.9 ± 0.3 |
| | AE11 | | − 37.1 ± 0.3 | − 37.8 ± 0.3 | − 35.2 ± 0.4 |
| | AE13 | − 38.5 ± 0.2 | − 38.6 ± 0.4 | − 38.7 ± 0.3 | − 37.9 ± 0.2 |
| | AE14 | − 35.6 ± 0.3 | − 35.9 ± 0.3 | − 36.7 ± 0.4 | − 35.6 ± 0.3 |

(~8.3‰) in lower estuary indicating intense recycling induced by tidal currents (Jennerjahn et al., 2008).

#### 5.2.2. Estimation of terrigenous versus aquatic productivity

The $P_{aq}$ provides the ability to differentiate submerged/floating aquatic macrophytes from emergent and terrestrial plant sources (Ficken et al., 2000). The non-emergent macrophytes display enhanced abundances of mid chain *n*-alkanes ($C_{21}$, $C_{23}$ and $C_{25}$), whereas emergent macrophytes have a distribution similar to those of terrestrial plants typically dominated by long chains (> $C_{27}$). The $P_{aq}$ < 0.1 corresponds to terrestrial plants, 0.1–0.4 to emergent macrophytes and 0.4–1 to submerged/floating macrophytes. The TAR reflects ratio between long-chain *n*-alkanes ($C_{27}$ + $C_{29}$ + $C_{31}$) to sum of short chain *n*-alkanes ($C_{15}$ + $C_{17}$ + $C_{19}$), which represent primary aquatic algae (both micro- and macro-algae) and photosynthetic bacteria (Bourbonniere and Meyers, 1996).

The inverse relation between TAR and $P_{aq}$ demonstrates that the terrigenous input was predominant in the upper estuary, which can be explained by the proximity to the Kallada River providing high concentrations of terrigenous *n*-alkanes (Fig. 3c and d). Conversely, the decreased TAR and increased $P_{aq}$ value reflects elevated marine productivity in the lower estuary. This interpretation has been supported by high annual gross productivity and faunal density in the lower Ashtamudi Estuary (Divakaran et al., 1981; Nair et al., 1984). Additionally, $\delta^{13}C_{org}$ values from the Ashtamudi sediments also demonstrate high deposition of river-derived OM in the upper estuary and an increasing portion of marine OM in the middle and lower parts of the estuary (Jennerjahn et al., 2008).

### 5.3. Source apportionment of OM

The $\delta^{13}C_{org}$ have been widely used for source apportionment of OM in the coastal systems (e.g., Sarma et al., 2011). However, the change in bulk $\delta^{13}C_{org}$ over time due to decomposition may provide an erroneous estimation of OM sources (Wang et al., 2008). The compound specific $\delta^{13}C$ values can refine the interpretation of bulk $\delta^{13}C_{org}$ data due to its higher resistance to degradation (Collister et al., 1994; Jaffé et al., 2001; Sikes et al., 2009). The $\delta^{13}C$ isotopic compositions of individual *n*-alkyl compounds largely depend on the differences in isotopic fractionation arise from the different carbon fixation pathways (e.g., Collister et al., 1994). $C_3$ plants are relatively $^{13}C$-depleted (*n*-$C_{24}$ to *n*-$C_{35}$ typically range from $\delta^{13}C$ = − 31‰ to − 39‰) and $C_4$ plants are $^{13}C$-enriched ($\delta^{13}C$ = − 18‰ to − 25‰).

The $\delta^{13}C$ values of the long-chain *n*-alkanes enables to distinguish relative OM contributions by $C_3$ versus $C_4$ plants at a given site using binary end-member mixing model (Zhang et al., 2003; Castañeda et al., 2009a; Garcin et al., 2014). The OM contributions from $C_3$ plants in Ashtamudi Estuary is mainly derived from the riverine transport of the dominant vegetation from the drainage basin of the Kallada River and the contribution from the mangrove plant litter in the upper Estuary. However, the $C_4$ plants contribution in the Ashtamudi Estuary encompasses contributions derived from terrestrial (riverine) and in-situ marine sources (e.g., sea grasses). The littoral zones of the south west coast of India is characterised by the presence of sea grasses (e.g., *Najas graminea*) (Nair et al., 1982). The sea grasses are characterised by $\delta^{13}C$ values similar to those of $C_4$ plants (Andrews and Abel, 1979; Benedict et al., 1980; Mead et al., 2005). Therefore, the obtained $C_4$ contribution has to be interpreted in terms of contribution derived from both terrestrial $C_4$ plants and/or marine sources. The $\delta^{13}C_{C31}$ average of modern $C_3$ (− 36.9 ± 1.5‰) and $C_4$ (− 21.0 ± 1.9‰) plants from the Ashtamudi region has been considered as end members. The relative contribution of the $C_3$ terrestrial plants and $C_4$ terrestrial plants and/or marine contribution can be calculated as follows;

$$\delta^{13}C = y^{*}(-36.9 \pm 1.5‰) + (1 - y)^{*}(-21.0 \pm 1.9‰)$$

(where y stands for the $C_3$ contribution).

The end-member estimation of Ashtamudi Estuary reveals dominance of $C_3$ terrestrial plants with values ranging from 83 ± 13% to 53 ± 8% (Supplementary material Table S5). This estimation agrees well with the $C_3$ plants dominated Kallada drainage basin (Jennerjahn et al., 2008). However, the spatial distribution of the terrestrial $C_3$ plants contribution shows decreasing values towards the marine dominated lower estuary (Fig. 4). This trend can be attributed to the OM contribution derived from marine sources. The high marine OM

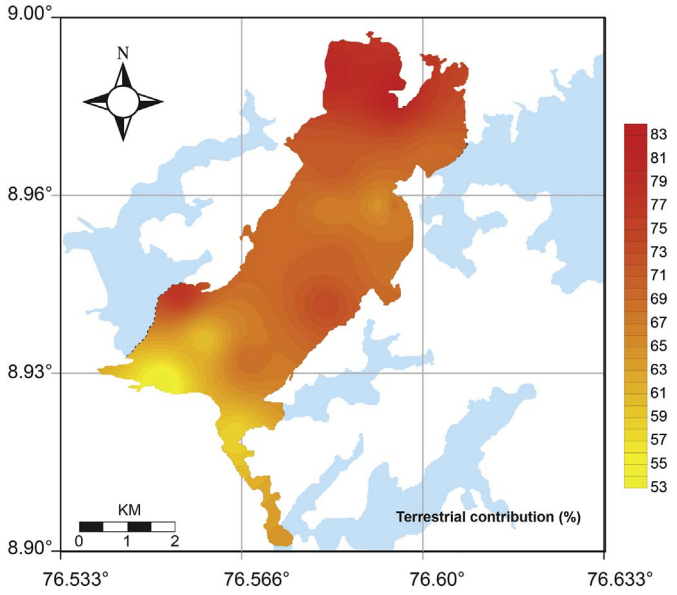


**Fig. 4.** Spatial representation of terrigenous contribution in Ashtamudi Estuary based on the end member modelling of compound specific $\delta^{13}C$ values.

contribution in the lower part of the estuary corroborates well with our *n*-alkane ($P_{aq}$ and TAR) proxies. A seaward increase in the marine OM contributions is consistent with a previous study based on $\delta^{13}C$ analysis of Ashtamudi sediments (Jennerjahn et al., 2008). The result clearly indicates the effectiveness of a coupled molecular and stable carbon isotope analysis for evaluating the OM sources in estuarine environments.

### 5.4. Implications for paleo-environmental reconstruction

The present study based on the *n*-alkane analysis in the surface sediments from the Ashtamudi Estuary allowed estimating the potential of different *n*-alkane indices. The various studies have used the shifts in long chain length (ACL or CPI) in sedimentary records for the assessment of paleovegetation and paleoclimate (e.g., Rommerskirchen et al., 2006; Kawamura et al., 2003; Castañeda et al., 2009b; Xue et al., 2016). The shifts in the longer chain *n*-alkanes are often interpreted in terms of changes in the plant community (Rommerskirchen et al., 2006; Schwark et al., 2002). Conversely, it has been suggested that a direct relationship exists between longer chain *n*-alkanes fluctuations and climatic conditions, for instance changing temperature (Kawamura et al., 2003; Castañeda et al., 2009a, 2009b) and increased aridity (Liu and Huang, 2005; Hoffmann et al., 2013; Tipple and Pagani, 2013). The result from the Ashtamudi Estuary suggests the need for cautious interpretation of shifts in the *n*-alkane distribution pattern as dominant factors controlling these parameters may be site-dependent. The robust application of *n*-alkane distributions as paleoclimate biomarkers require the systematic survey of different modern plants and sediments from the region. Our results underline the need of regional calibrations of the *n*-alkane distribution for paleoclimate reconstruction.

The modern calibration from Ashtamudi Estuary provides potential in using *n*-alkane distribution in conjunction with carbon isotope as part of a high-resolution multi-proxy paleoclimate reconstruction from the region. The modern spatial distribution in Ashtamudi Estuary is caused by the relationship between riverine inputs and the extent of tidal penetration, deposition and reworking. Thus, a downcore record of the organic proxies from the Ashtamudi Estuary could reflect the changes in fresh water discharge and sea level fluctuations. This study represents a very valuable future application of lipid biomarkers on sediments cores from the region. Being the first of its kind in Indian subcontinent, this study would be beneficial for interpreting signals retained in molecular level to interpret past changes in climate, vegetation and the carbon cycle in the estuarine environment.

## 6. Conclusions

Lipid (*n*-alkane) distribution and compound-specific $\delta^{13}C$ analyses were used to identify organic matter sources and distribution in tropical Ashtamudi Estuary, Southern India. We evaluated the applicability of *n*-alkane indices to assess the relative contribution of terrestrial versus marine organic matter inputs to the estuarine environment. The *n*-alkane indices of surface sediments from Ashtamudi Estuary demonstrate a shift in OM sources along the NE to SW transect from mangrove influenced upper estuary to plankton/seagrass dominated lower estuary. The CPI and ACL values demonstrate high terrestrial *n*-alkane concentrations proximal to the river sources, whereas TAR and $P_{aq}$ reveals OM contribution derived from marine sources. The quantitative source apportionment calculated using carbon isotope end-members indicates dominance of terrestrial $C_3$ contribution in the Ashtamudi Estuary. The results of this study have great significance for interpreting organic matter sources in modern and ancient tropical coastal environments.

## Acknowledgements

The biomarker analyses were performed at Stable Isotope Laboratory (Silika Lab), Indian Institute of Science Education and Research, Kolkata. AA, YA and PK are thankful to the Director, Indian Institute of Science Education and Research Mohali (IISER-M) and Convenor, Department of Earth and Environmental Science for their support and encouragements. AA and PKM gratefully acknowledge the financial support provided by Inspire Fellowship from Department of Science and Technology. YA and PK thanks IISER-M for the financial support provided for biomarker analyses.

Supplementary data to this article can be found online at http://dx.doi.org/10.1016/j.marchem.2017.08.002.

## References

Ahad, J.M., Ganeshram, R.S., Bryant, C.L., Cisneros-Dozal, L.M., Ascough, P.L., Fallick, A.E., Slater, G.F., 2011. Sources of *n*-alkanes in an urbanized estuary: insights from molecular distributions and compound-specific stable and radiocarbon isotopes. Mar. Chem. 126, 239–249.

Aichner, B., Herzschuh, U., Wilkes, H., 2010. Influence of aquatic macrophytes on the stable carbon isotopic signatures of sedimentary organic matter in lakes on the Tibetan Plateau. Org. Geochem. 41, 706–718.

Andrews, T.J., Abel, K.M., 1979. Photosynthetic carbon metabolism in seagrasses $^{14}C$-labeling evidence for the $C_3$ pathway. Plant Physiol. 63, 650–656.

Anooja, S., Padmalal, D., Maya, K., Mohan, S.V., Baburaj, B., 2013. Heavy mineral contents and provenance of Late Quaternary sediments of southern Kerala, Southwest India. IJMS 42, 749–757.

Antony, M.M., Ignatius, J., 2016. A hydrological study of Ashtamudi Lake, Kerala, India with special reference to its ecological difference. Int. J. Sci. Res. 5, 1841–1846.

Babu, K.N., Omana, P.K., Mohan, M., 2010. Water and sediment quality of Ashtamudi estuary, a Ramsar site, southwest coast of India—a statistical appraisal. Environ. Monit. Assess. 165, 307–319.

Basu, S., Anoop, A., Sanyal, P., Singh, P., 2017. Lipid distribution in the lake Ennamangalam, south India: indicators of organic matter sources and paleoclimatic history. Quat. Int. 443, 238–247.

Benedict, C.R., Wong, W.W., Wong, J.H., 1980. Fractionation of the stable isotopes of inorganic carbon by seagrasses. Plant Physiol. 65, 512–517.

Bianchi, T.S., 2006. Biogeochemistry of Estuaries. Oxford University Press.

Bianchi, T.S., Allison, M.A., 2009. Large-river delta-front estuaries as natural "recorders" of global environmental change. Proc. Natl. Acad. Sci. 106, 8085–8092.

Bourbonniere, R.A., Meyers, P.A., 1996. Sedimentary geolipid records of historical changes in the watersheds and productivities of Lakes Ontario and Erie. Limnol. Oceanogr. 41, 352–359.

Bray, E.E., Evans, E.D., 1961. Distribution of *n*-paraffins as a clue to recognition of source beds. Geochim. Cosmochim. Acta 22, 2–15.

Burton, J.D., Liss, P.S., 1976. Estuarine Chemistry. Academic press, London.

Bush, R.T., McInerney, F.A., 2013. Leaf wax n-alkane distributions in and across modern plants: implications for paleoecology and chemotaxonomy. Geochim. Cosmochim. Acta 117, 161–179.

Castañeda, I.S., Mulitza, S., Schefuß, E., dos Santos, R.A.L., Damsté, J.S.S., Schouten, S., 2009a. Wet phases in the Sahara/Sahel region and human migration patterns in

North Africa. Proc. Natl. Acad. Sci. 106, 20159–20163.
Castañeda, I.S., Werne, J.P., Johnson, T.C., Filley, T.R., 2009b. Late Quaternary vegetation history of southeast Africa: the molecular isotopic record from Lake Malawi. Palaeogeogr. Palaeoclimatol. Palaeoecol. 275, 100–112.
Champion, H.G., Seth, S.K., 1968. A Revised Survey of the Forest Types of India. Government of India, New Delhi.
Chevalier, N., Savoye, N., Dubois, S., Lama, M.L., David, V., Lecroart, P., le Ménach, K., Budzinski, H., 2015. Precise indices based on n-alkane distribution for quantifying sources of sedimentary organic matter in coastal systems. Org. Geochem. 88, 69–77.
Collister, J.W., Rieley, G., Stern, B., Eglinton, T., Fry, B., 1994. Compound specific $\delta^{13}C$ analyses of leaf lipids from plants with differing carbon dioxide mechanisms. Org. Geochem. 21, 619–627.
Cranwell, P.A., 1973. Chain-length distribution of n-alkanes from lake sediments in relation to post-glacial environmental change. Freshw. Biol. 3, 259–265.
Cranwell, P.A., Eglinton, G., Robinson, N., 1987. Lipids of aquatic organisms as potential contributors to lacustrine sediments-II. Org. Geochem. 11, 513–527.
Divakaran, O., Murugan, T., Nair, N.B., 1981. Distribution and seasonal variation of the benthic fauna of the Ashtamudi lake, south-west coast of India. Mahasagar 14, 167–172.
Eglinton, T.I., Eglinton, G., 2008. Molecular proxies for paleoclimatology. Earth Planet. Sci. Lett. 275, 1–16.
Eglinton, G., Hamilton, R.J., 1963. The distribution of alkanes. In: Swain, T. (Ed.), Chemical Plant Taxonomy. Academic Press, London, pp. 187–218.
Farrington, J.W., Tripp, B.W., 1977. Hydrocarbons in western North Atlantic surface sediments. Geochim. Cosmochim. Acta 41, 1627–1641.
Fellman, J.B., Hood, E., Edwards, R.T., D'Amore, D.V., 2009. Changes in the concentration, biodegradability, and fluorescent properties of dissolved organic matter during stormflows in coastal temperate watersheds. J. Geophys. Res. 114 (G1).
Ficken, K.J., Li, B., Swain, D.L., Eglinton, G., 2000. An *n*-alkane proxy for the sedimentary input of submerged/floating freshwater aquatic macrophytes. Org. Geochem. 31, 745–749.
Gagosian, R.B., Peltzer, E.T., 1986. The importance of atmospheric input of terrestrial organic material to deep sea sediments. Org. Geochem. 10, 661–669.
Garcin, Y., Schefuß, E., Schwab, V.F., Garreta, V., Gleixner, G., Vincens, A., Todou, G., Séné, O., Onana, J.M., Achoundong, G., Sachse, D., 2014. Reconstructing $C_3$ and $C_4$ vegetation cover using *n*-alkane carbon isotope ratios in recent lake sediments from Cameroon, Western Central Africa. Geochim. Cosmochim. Acta 142, 482–500.
Ghosh, S., Sanyal, P., Kumar, R., 2017. Evolution of $C_4$ plants and controlling factors: insight from n-alkane isotopic values of NW Indian Siwalik paleosols. Org. Geochem. 110, 110–121.
Harvey, H.R., Mannino, A., 2001. The chemical composition and cycling of particulate and macromolecular dissolved organic matter in temperate estuaries as revealed by molecular organic tracers. Org. Geochem. 32, 527–542.
He, Y., Zheng, Y., Pan, A., Zhao, C., Sun, Y., Song, M., Zheng, Z., Liu, Z., 2014. Biomarker-based reconstructions of Holocene lake-level changes at Lake Gahai on the northeastern Tibetan Plateau. The Holocene 24, 405–412.
Hedges, J.I., Prahl, F.G., 1993. Early diagenesis: consequences for applications of molecular biomarkers. In: Engel, M.H., Macko, S.A. (Eds.), Organic Geochemistry: Principles and Applications. Plenum Press, New York, pp. 237–253.
Hoffmann, B., Kahmen, A., Cernusak, L.A., Arndt, S.K., Sachse, D., 2013. Abundance and distribution of leaf wax n-alkanes in leaves of Acacia and Eucalyptus trees along a strong humidity gradient in northern Australia. Org. Geochem. 62, 62–67.
Jaffé, R., Mead, R., Hernandez, M.E., Peralba, M.C., DiGuida, O.A., 2001. Origin and transport of sedimentary organic matter in two subtropical estuaries: a comparative, biomarker-based study. Org. Geochem. 32, 507–526.
Jeng, W.L., 2006. Higher plant n-alkane average chain length as an indicator of petrogenic hydrocarbon contamination in marine sediments. Mar. Chem. 102, 242–251.
Jennerjahn, T.C., Soman, K., Ittekkot, V., Nordhaus, I., Sooraj, S., Priya, R.S., Lahajnar, N., 2008. Effect of land use on the biogeochemistry of dissolved nutrients and suspended and sedimentary organic matter in the tropical Kallada River and Ashtamudi estuary, Kerala, India. Biogeochemistry 90, 29–47.
Johannessen, T., Dahl, E., 1996. Declines in oxygen concentrations along the Norwegian Skagerrak coast, 1927–1993: a signal of ecosystem changes due to eutrophication? Limnol. Oceanogr. 41, 766–778.
Kawamura, K., Ishimura, Y., Yamazaki, K., 2003. Four years' observations of terrestrial lipid class compounds in marine aerosols from the western North Pacific. Glob. Biogeochem. Cycles 17, 1–19.
Kennicutt II, M.C., Barker, C., Brooks, J.M., DeFreitas, D.A., Zhu, G.H., 1987. Selected organic matter source indicators in the Orinoco, Nile and Changjiang deltas. Org. Geochem. 11, 41–51.
Kolattukudy, P.E., 1976. Introduction to natural waxes. In: Chemistry and Biochemistry of Natural Waxes. Elsevier Scientific Pub. Co.
Krishnan, J.U., Saroja Devi, S., Jithine, J.R., Ajesh, G., Lekshmi, N.R., 2014. Status of *sonneratia alba* (mangrove apple) from the ashtamudi lake, kerala, India. J. Aquat. Biol. Fish. 2, 237–240.
Liu, W., Huang, Y., 2005. Compound specific D/H ratios and molecular distributions of higher plant leaf waxes as novel paleoenvironmental indicators in the Chinese Loess Plateau. Org. Geochem. 36, 851–860.
Mead, R., Xu, Y., Chong, J., Jaffé, R., 2005. Sediment and soil organic matter source assessment as revealed by the molecular distribution and carbon isotopic composition of *n*-alkanes. Org. Geochem. 36, 363–370.
Meyers, P.A., 2003. Applications of organic geochemistry to paleolimnological reconstructions: a summary of examples from the Laurentain Great Lakes. Org. Geochem. 34, 261–289.
Meyers, P.A., Ishiwatari, R., 1993. Lacustrine organic geochemistry—an overview of indicators of organic matter sources and diagenesis in lake sediments. Org. Geochem. 20, 867–900.
Middelburg, J.J., Herman, P.M., 2007. Organic matter processing in tidal estuaries. Mar. Chem. 106, 127–147.
Müller, A., 2001. Late-and postglacial sea-level change and paleoenvironments in the Oder Estuary, Southern Baltic Sea. Quat. Res. 55, 86–96.
Nair, N.B., Sobha, V., Arunachalam, M., 1982. Algae from southern Kerala coast. Indian J. Mar. Sci. 11, 266–269.
Nair, N.B., Azis, P.A., Dharmaraj, K., Arunachalam, M., Kumar, K.K., Balasubramanian, N.K., 1984. Ecology of Indian estuaries—V: primary productivity of the Ashtamudi estuary, south-west coast of India. Proc. Anim. Sci. 93, 9–23.
Nair, K.M., Padmalal, D., Kumaran, K.P.N., Sreeja, R., Limaye, R.B., Srinivas, R., 2010. Late quaternary evolution of Ashtamudi–Sasthamkotta lake systems of Kerala, south west India. J. Asian Earth Sci. 37, 361–372.
Padmalal, D., Kumaran, K.P.N., Nair, K.M., Baijulal, B., Limaye, R.B., Mohan, S.V., 2011. Evolution of the coastal wetland systems of SW India during the Holocene: evidence from marine and terrestrial archives of Kollam coast, Kerala. Quat. Int. 237, 123–139.
Poynter, J., Eglinton, G., 1990. Molecular composition of three sediments from hole 717c: the Bengal fan. In: Proceedings of the Ocean Drilling Program: Scientific Results. 116. pp. 155–161.
Poynter, J.G., Farrimond, P., Robinson, N., Eglinton, G., 1989. Aeolian-derived higher plant lipids in the marine sedimentary record: links with palaeoclimate. In: Paleoclimatology and Paleometeorology: Modern and Past Patterns of Global Atmospheric Transport. Springer, Netherlands, pp. 435–462.
Qasim, S.Z., 2003. Indian Estuaries. Allied Publications Pvt. Ltd, Heriedia Marg, Ballard Estate, Mumbai 259 pp.
Ranjan, R.K., Routh, J., Klump, J.V., Ramanathan, A.L., 2015. Sediment biomarker profiles trace organic matter input in the Pichavaram mangrove complex, southeastern India. Mar. Chem. 171, 44–57.
Resmi, P., Manju, M.N., Gireeshkumar, T.R., Kumar, C.R., Chandramohanakumar, N., 2016. Source characterisation of sedimentary organic matter in mangrove ecosystems of northern Kerala, India: inferences from bulk characterisation and hydrocarbon biomarkers. Regional Studies in Marine Science 7, 43–54.
Rieley, G., Collier, R.J., Jones, D.M., Eglinton, G., 1991. The biogeochemistry of Ellesmere Lake, U.K.—I: source correlation of leaf wax inputs to the sedimentary lipid record. Org. Geochem. 17, 901–912.
Rommerskirchen, F., Eglinton, G., Dupont, L., Güntner, U., Wenzel, C., Rullkötter, J., 2003. A north to south transect of Holocene southeast Atlantic continental margin sediments: relationship between aerosol transport and compound-specific $\delta^{13}C$ land plant biomarker and pollen records. Geochem. Geophys. Geosyst. 4, 1101–1128.
Rommerskirchen, F., Plader, A., Eglinton, G., Chikaraishi, Y., Rullkötter, J., 2006. Chemotaxonomic significance of distribution and stable carbon isotopic composition of long-chain alkanes and alkan-1-ols in C4 grass waxes. Org. Geochem. 37, 1303–1332.
Sabu, T., Ambat, B., 2007. Floristic analysis of wetlands of Kerala. In: Proceedings of the Kerala Environment Congress, pp. 91–105.
Sajan, K., Damodaran, K.T., Flemming, W.B., 1992. The sedimentary frame work of the Ashtamudi estuary, Kerala, South West India. Zentralblatt für Geologie und Paläontologie, Teil I H12, 2995–3007.
Samanta, A., Bera, M.K., Ghosh, R., Bera, S., Filley, T., Pande, K., Rathore, S.S., Rai, J., Sarkar, A., 2013. Do the large carbon isotopic excursions in terrestrial organic matter across Paleocene–Eocene boundary in India indicate intensification of tropical precipitation? Palaeogeogr. Palaeoclimatol. Palaeoecol. 387, 91–103.
Saran, H.M., Adoni, A.D., 1982. Studies on seasonal variations in pH and dissolved oxygen contents in Sagar Lake. Acta Bot. Ind. 10, 324–328.
Sarkar, S., Wilkes, H., Prasad, S., Brauer, A., Riedel, N., Stebich, M., Basavaiah, N., Sachse, D., 2014. Spatial heterogeneity in lipid biomarker distributions in the catchment and sediments of a crater lake in central India. Org. Geochem. 66, 125–136.
Sarma, V.V.S.S., Kumar, N.A., Prasad, V.R., Venkataramana, V., Appalanaidu, S., Sridevi, B., Kumar, B.S.K., Bharati, M.D., Subbaiah, C.V., Acharyya, T., Rao, G.D., 2011. High $CO_2$ emissions from the tropical Godavari estuary (India) associated with monsoon river discharges. Geophys. Res. Lett. 38 (8).
Schouten, S., Woltering, M., Rijpstra, W.I.C., Sluijs, A., Brinkhuis, H., Damsté, J.S.S., 2007. The Paleocene–Eocene carbon isotope excursion in higher plant organic matter: differential fractionation of angiosperms and conifers in the Arctic. Earth Planet. Sci. Lett. 258, 581–592.
Schwark, L., Zink, K., Lechterbeck, J., 2002. Reconstruction of postglacial to early Holocene vegetation history in terrestrial Central Europe via cuticular lipid biomarkers and pollen records from lake sediments. Geology 30, 463–466.
Seki, O., Yoshikawa, C., Nakatsuka, T., Kawamura, K., Wakatsuchi, M., 2006. Fluxes, source and transport of organic matter in the western Sea of Okhotsk: stable carbon isotopic ratios of n-alkanes and total organic carbon. Deep-Sea Res. I Oceanogr. Res. Pap. 53, 253–270.
Sikes, E.L., Uhle, M.E., Nodder, S.D., Howard, M.E., 2009. Sources of organic matter in a coastal marine environment: evidence from *n*-alkanes and their $\delta^{13}C$ distributions in the Hauraki Gulf, New Zealand. Mar. Chem. 113, 149–163.
Simoneit, B.R., Cardoso, J.N., Robinson, N., 1991. An assessment of terrestrial higher molecular weight lipid compounds in aerosol particulate matter over the South Atlantic from about 30–70 S. Chemosphere 23, 447–465.
Sujatha, C.H., Nify, B., Ranjitha, R., Fanimol, C.L., Samantha, N.K., 2009. Nutrient dynamics in the two lakes of Kerala, India. Indian Journal of Marine Sciences 38, 451–456.
Sumesh, C., Benno Pereira, F.G., Sini Wilson, S., Vishnu, S.R., 2014. Distribution of mangroves in the ashtamudi estuary. J. Aquat. Biol. Fish. 2, 310–312.
Thornton, S.F., McManus, J., 1994. Application of organic carbon and nitrogen stable isotope and C/N ratios as source indicators of organic matter provenance in estuarine systems: evidence from the Tay Estuary, Scotland. Estuar. Coast. Shelf Sci. 38,

219–233.
Tipple, B.J., Pagani, M., 2013. Environmental control on eastern broadleaf forest species' leaf wax distributions and D/H ratios. Geochim. Cosmochim. Acta 111, 64–77.
Wang, G., Feng, X., Han, J., Zhou, L., Tan, W., Su, F., 2008. Paleovegetation reconstruction using $\delta^{13}C$ of soil organic matter. Biogeosci. Discuss. 5, 1795–1823.
Wang, Y., Liu, D., Richard, P., Li, X., 2013. A geochemical record of environmental changes in sediments from Sishili Bay, northern Yellow Sea, China: anthropogenic influence on organic matter sources and composition over the last 100 years. Mar. Pollut. Bull. 77, 227–236.
Xue, J., Dang, X., Tang, C., Yang, H., Xiao, G., Meyers, P.A., Huang, X., 2016. Fidelity of plant-wax molecular and carbon isotope ratios in a Holocene paleosol sequence from the Chinese Loess Plateau. Org. Geochem. 101, 176–183.
Zhang, Z., Zhao, M., Lu, H., Faiia, A.M., 2003. Lower temperature as the main cause of $C_4$ plant declines during the glacial periods on the Chinese Loess Plateau. Earth Planet. Sci. Lett. 214, 467–481.